Disruption of Visual and Motor Connectivity in Spinocerebellar Ataxia Type 7

Carlos R. Hernandez-Castillo, PhD,[1,2] Sarael Alcauter, PhD,[2] Victor Galvez, MSci,[1] Fernando A. Barrios, PhD,[3] Petra Yescas, PhD,[4] Adriana Ochoa, Msci,[4] Lizbeth Garcia, MSci,[4] Rosalinda Diaz, MSci,[5] Wei Gao, PhD,[2*] and Juan Fernandez-Ruiz, PhD[1,5,6*]

[1]Instituto de Neuroetologia, Universidad Veracruzana, Xalapa, Mexico
[2]Department of Radiology and BRIC, University of North Carolina, Chapel Hill, North Carolina, USA
[3]Instituto de Neurobiología, Universidad Nacional Autónoma de México, Mexico City, Mexico
[4]Departamento de Neurogenetica y Biologia Molecular, Instituto Nacional de Neurologia y Neurocirugia. Manuel Velasco Suarez, Mexico City, Mexico
[5]Departamento de Fisiologia, Facultad de Medicina, Universidad Nacional Autonoma de Mexico, Mexico City, Mexico
[6]Facultad de Psicologia, Universidad Veracruzana, Xalapa, Mexico

ABSTRACT: Spinocerebellar ataxia type 7 (SCA7) is an autosomal-dominant neurodegenerative disorder characterized by progressive ataxia and retinal dystrophy. It is caused by a CAG trinucleotide expansion in the *ataxin7* gene. Anatomical studies have shown severe cerebellar degeneration and region-specific neocortical atrophy in SCA7 patients. However, the impact of the neurodegeneration on the functional integration of the remaining tissue is still unknown. The aim of this study was to examine functional connectivity abnormalities in areas with significant gray matter atrophy in SCA7 patients and their relationship with number of CAG repeats. Using a combination of voxel-based morphometry and resting-state fMRI, we studied 26 genetically confirmed SCA7 patients and aged-matched healthy controls. In SCA7 patients we found reduced functional interaction between the cerebellum and the middle and superior frontal gyri, disrupted functional connectivity between the visual and motor cortices, and increased functional coordination between atrophied areas of the cerebellum and a range of visual cortical areas compared with healthy controls. The degree of mutation expansion showed a negative effect on both the functional interaction between the right anterior cerebellum and the left superior frontal gyrus and the connectivity between the right anterior cerebellum and left parahippocampal gyrus. We found abnormal functional connectivity patterns, including both hypo- and hyper-connectivity, compared with controls. These abnormal patterns show reasonable association with the severity of gene mutation. Our findings suggest that aberrant changes are prevalent in both motor and visual systems, adding significantly to our understanding of the pathophysiology of SCA7. © 2013 *Movement* Disorder Society

Key Words: spinocerebellar ataxia 7; functional connectivity; visual network; motor network; frontocerebellar network

---

Spinocerebellar ataxias (SCAs) are a group of autosomal-dominant cerebellar ataxias (ADCAs) that are classified according to specific genetic mutations. Among these, the CAG trinucleotide expansion in the coding region of the *ataxin7* gene located on chromosome 3p21 causes SCA7,[1] which is considered one of the rarest forms of genetically ADCAs.[2] In healthy subjects the CAG codon is repeated between 3 and 35 times in the *ataxin7* locus, whereas SCA7 patients have 36 or more CAG repeats.[3,4] The neuropathological deterioration varies as a function of the number of CAG repeats; for example, when the number of CAG repeats is between 36 and 43, the degenerative process is slow, with few or no retinal abnormalities.[5] Clinically, SCA7 is characterized by a combination of cerebellar ataxia and macular degeneration and is the only spinocerebellar ataxia that manifests itself in permanent blindness.[6–8] However, patients may eventually develop other neurological deficits, including loss of manual dexterity, speech dysarthria, dysphagia, and eye movement abnormalities.[2] A number of neuropathological studies have documented the anatomical consequences of the neurodegenerative process. These include severe degeneration of the cerebellar cortex and other cortical regions.[9–14]

However, there is a profound lack of information regarding the functional changes in the brain that occur as a result of the SCA7 degenerative process. Unlike other neurodegenerative diseases such as Alzheimer's or Parkinson's disease,[15,16] for which functional wiring abnormalities have been extensively studied, few studies have addressed SCAs,[17–19] and none have been conducted on SCA7 to elucidate the related functional abnormalities. By measuring the temporal synchronization among distant brain areas, the resting-state functional magnetic resonance imaging (rsfMRI) technique[20] emerges as a powerful tool for delineating the brain's intrinsic functional wiring architecture and has been successfully applied to study various neurodegenerative diseases and psychiatric disorders.[21,22] Specifically, rsfMRI studies in patients with autism spectrum disorders have suggested that the disease is characterized by alterations in resting-state connectivity, showing frontal disruptions.[23,24] Disruptions within the default mode network have been reported in patients suffering from Alzheimer's disease, mild cognitive impairment,[25–29] and widespread abnormal patterns in schizophrenia.[30] Given the well-documented structural atrophy related to SCA7, the use of rsfMRI to delineate its functional circuitry abnormalities represents a promising way to elucidate the neurophysiological underpinnings of this rare disease.

Patients and Methods

Subjects

Twenty-six patients with a molecular diagnosis of spinocerebellar ataxia type 7 and a CAG expansion score higher than 40[31] participated in this study (11 women; right-handed; mean age ± SD, 39.4 ± 14.7 years; complete information for each patient is in Supplementary Table S1). Twenty-six healthy volunteers formed the control group and were age- and sex-matched to the SCA7 patients (11 women; right-handed; mean age, 38.46 years). No history of any neurological diseases, psychiatric disorders, or neuropharmacological treatment was reported in all normal controls. No significant difference in age between the groups was found (two-group *t* test, *P* = 0.82). All participants gave their informed consent before entering the study. All procedures in this study were conducted in accordance with the international standards laid down in the Helsinki Declaration of 1964. The procedures carried out were in accordance with the ethical standards of the committees on human experimentation of the Universidad Nacional Autonoma de Mexico.

Image Acquisition

All images were acquired using a 3.0-T Achieva MRI scanner (Phillips Medical Systems, Eindhoven, Holland). The anatomical acquisition consisted of a 3-D T1 Fast Field-Echo sequence, with TR/TE of 8/3.7 ms, FOV of 256×256 mm; and an acquisition and reconstruction matrix of 256×256, resulting in an isometric resolution of $1 \times 1 \times 1$ mm. Functional images were collected using an Echo Planar Imaging single-shot sequence with a TR of 2000 ms, TE of 35 ms, and 120 whole-brain volumes with 34 slices. Final isometric resolution of the structural images was $3 \times 3 \times 4$ mm without gaps. During functional MRI acquisition, subjects in all groups were instructed to keep their eyes closed, to think about nothing in particular, and to stay awake. Five dummy scans were performed at the beginning of each functional acquisition to allow magnetization to reach a steady state.

Preprocessing

RsfMRI preprocessing included brain extraction, time shifting, motion correction, spatial smoothing (6 mm full-width at half-maximum Gaussian kernel), linear trend removal, and temporal filtering (band pass, 0.01-0.08 Hz) using FSL (FMRIB, Oxford University, Oxford, UK). A regression technique was used to remove sources of variance including white matter, cerebrospinal fluid, and global mean signal.[32] Moreover, we implemented a new method[33] to further control motion artifacts with a signal change < 0.5% and a frame-wise displacement of 0.5 mm. All structural images were warped to the Montreal Neurological Institute MNI template using the nonlinear registration method.[34–36] After rigid alignment of rsfMRI images to structural images, spatial normalization of rsfMRI images to the MNI template was achieved

TABLE 1. Location of seeds used for connectivity analysis

Side	Anatomical region	MNI coordinates		
		X	Y	Z
Right	Cerebellum anterior	36	−58	−28
Left	Cerebellum anterior	−24	−66	−24
Right	Cerebellum posterior	32	−72	−40
Left	Cerebellum posterior	−16	−74	−42
Right	Lingual gyrus	18	−92	−10
Left	Inferior occipital gyrus	−30	−92	−12
Right	Cuneus	18	−72	28
Left	Precuneus	−22	−74	32
Right	Precentral gyrus	48	−10	42
Left	Precentral gyrus	−48	−12	44
Right	Postcentral gyrus	46	−22	40
Left	Postcentral gyrus	−44	−16	32

using the transformation field acquired during the structural image registration.

Voxel-Based Morphometry Analysis to Detect Structural Atrophy Areas as Seeds

Voxel-based morphometry (VBM) analysis[37,38] was performed using FSL-VBM.[39] After smoothing with a Gaussian isotropic kernel of 2 mm sigma on the two group structural images (in MNI space), a two-sample t test was applied, and significance was defined as $P < 0.05$ after correcting for multiple comparisons using the randomized permutation method[40,41] (Supplementary Fig. 1). VBM analysis showed a high degree of gray matter atrophy in SCA7 patients compared with healthy controls. The right anterior cerebellum showed the greatest amount of atrophy, followed by the left posterior cerebellum. We selected specific brain areas related to the motor and visual deficits in SCA7. To this end and based on the local maxima of the resulting t-map, a total of 12 regions of interest (ROIs; 12-mm sphere centered at the local maxima) were defined in which SCA7 patients showed gray matter volume reduction (Table 1). No areas were detected to show significantly increased gray matter volume in SCA7 patients compared with healthy controls.

Functional Connectivity Analysis

Using MATLAB R2012a (The Mathworks, Inc., Natick, MA), the mean time course of each defined seed was extracted by calculating the average of all voxels within the 12-mm sphere. Functional connectivity maps were created by calculating a Pearson's linear correlation between the seed's average signal and every other voxel in the whole brain. Besides defining the significant map of each seed for both groups using a voxel-wise two-way t test, a two-sample t test was performed between SCA7 and control functional connectivity maps to detect significant differences. To control type I error in this analysis,

Monte Carlo simulations were performed using the AFNI 3dClustSim program (parameters were individual voxel $P = 0.01$, 20,000 simulations, FWHM 6 mm, with mask of the whole brain), providing a combined individual voxel probability threshold and cluster size threshold,[42] and a corrected significance level of $P < 0.05$ was obtained by selecting clusters with a minimum volume of 1152 mm^3 at an uncorrected individual voxel height threshold of $P < 0.01$. To test the association with genetic mutation severity and clinical symptoms, a general linear model (GLM) analysis was conducted using detected functional connectivity abnormalities as the independent variable and CAG expansion score and number of years after symptoms onset as dependent variables. Age and sex were included as covariates.

Results

Functional Connectivity Abnormalities

Functional connectivity analysis of all the seeds revealed 54 regions showing significant differences in functional interactions with corresponding seeds between healthy controls and SCA7 patients ($P < 0.01$, minimal cluster size 20 voxels). The most significant differences are shown in Figure 1. The largest functional connectivity increases in SCA7 patients were found between the right lingual gyrus seed and right posterior cerebellum and vice versa. The largest functional connectivity decreases were found between the right posterior cerebellum seed and left superior frontal gyrus (BA 6), the right anterior cerebellum seed and right superior frontal gyrus (BA 10), the right lingual gyrus seed and bilateral postcentral gyri (BA 3), the left precentral gyrus seed and left lingual gyrus (BA 18), and the right precuneus seed and right inferior frontal gyrus (BA 44). The complete list of significant functional connectivity differences in the patients can be found in Table 2 (significant functional connectivity increase) and Table 3 (significant functional connectivity decrease).

Association With Genetic Mutation and Years After Onset

Three significant effects were detected in this GLM association analysis. Specifically, the degree of CAG expansion had a negative effect on the functional connectivity between the right anterior cerebellum and left superior frontal gyrus ($t = −3.22$, $P = 0.004$ uncorrected; Fig. 2, top) and between the right anterior cerebellum and left parahippocampal gyrus ($t = −2.25$, $P = 0.03$ uncorrected; Fig. 2, center). The number of years after symptom onset also had a significant effect on the functional connectivity between the right anterior cerebellum and left superior frontal gyrus ($t = −2.84$, $P = 0.01$ uncorrected; Fig. 2, bottom).
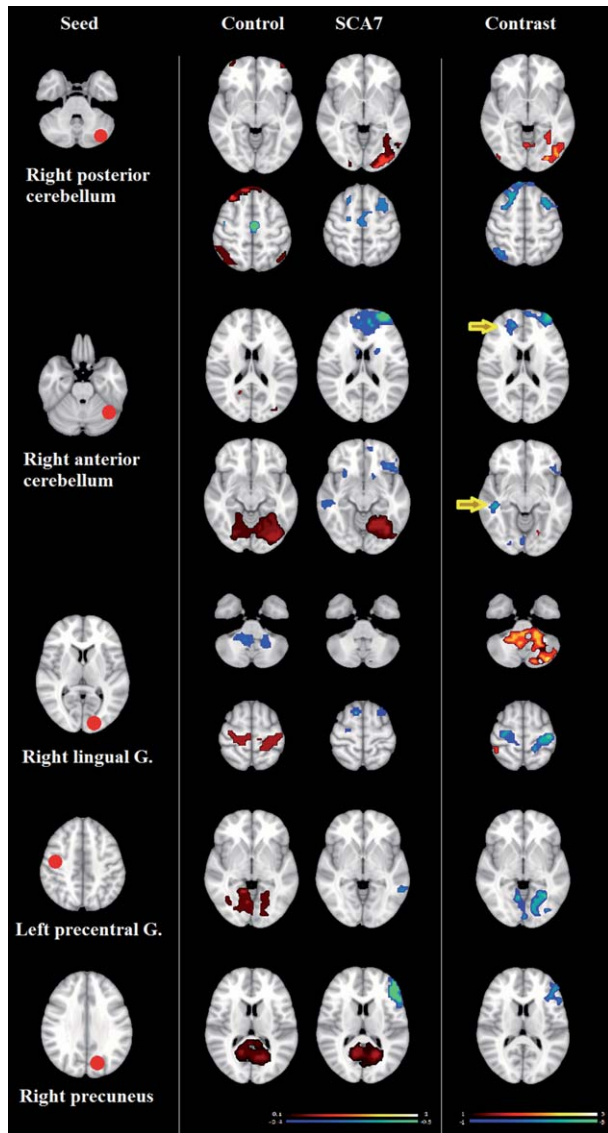
FIG. 1. Functional connectivity maps for seeds in right posterior cerebellum, right anterior cerebellum, right lingual gyrus, left precentral gyrus, and right precuneus. Left column represents the location of seeds; center column shows the mean functional connectivity maps (threshold $P < 0.01$ uncorrected) with warm colors representing positive correlations and cold colors negative correlations; and right column shows the t-maps resulting from the t test between groups (threshold $P < 0.05$ corrected see Methods). Warm colors represent increases in connectivity and cold colors decreases in connectivity in SCA7 compared with controls. Yellow arrows indicate brain regions where CAG expansion has a negative effect on functional connectivity strength (see "Association With Genetic Mutation and Years After Onset" in the Results section). [Color figure can be viewed in the online issue, which is available at wileyonlinelibrary.com.]

Discussion

In this study, we explored the functional wiring abnormalities associated with structural deficits in the rare neurodegenerative disease SCA7. Our findings indicate widespread abnormalities in the functional interaction pattern associated with structurally atrophied areas, including both hyper- and hypoconnectiv-

ity. Specifically, our results highlight the reduction of cerebellar-frontal and visual-motor functional connectivity as well as the enhancement of cerebellar-visual connectivity. Moreover, our results suggest that abnormalities associated with the functional circuit centered at the right anterior cerebellum area are associated with the severity of genetic mutation and symptoms.

Abnormality in Cerebellar Functional Connectivity

Patients with SCA7 showed widespread functional connectivity abnormalities within cerebellum-centered circuits. The cerebellum contributes to both motor and nonmotor function[43] and receives input from a wide variety of sources, including areas of the frontal, prefrontal, cingulate, and posterior parietal cortex. It is thought that this information is funneled into the motor system to generate and control movement.[44,45] However, all previous studies have focused on the structural deficits associated with the cerebellum, whereas potential functional connectivity abnormalities remain unknown. In the current study we delineated for the first time the functional interaction abnormalities associated with the cerebellum, a critical structure in SCA7 neurodegeneration.[14]

Specifically, a functional connectivity increase was observed mainly between the cerebellum and the right lingual gyrus and also between the cerebellum and the inferior/middle occipital gyrus when comparing the SCA7 group with normal controls. Interestingly, both areas showed significant gray matter atrophy associated with SCA7.[14] Given previous reports that an increase in functional connectivity may allow structurally atrophied brain regions to remain functional,[46–48] this enhanced connectivity between the cerebellum and visual areas may reflect a compensatory mechanism. In the same way we found increased connectivity between the cerebellum and precuneus and parietal cortices, regions related to sensory integration,[49] and between the cerebellum and the hippocampus, associated with spatial memory and navigation,[50] suggesting compensation by these regions during structural degeneration. This compensatory hypothesis is also consistent with the observation that the cerebellum may compensate, in part, for disrupted visual-motor coordination (discussed below). On the other hand, disrupted connectivity with atrophied areas of the cerebellum was observed in several frontal regions and the parahippocampal area (BA 36); see Table 2. Previous studies have mapped the close functional connectivity between the frontal lobe and the cerebellum and have indicated the importance of these connections in different cognitive operations such as self-monitoring and verbal memory.[51,52] Moreover, functional changes in the parahippocampal area have been frequently reported to coincide with changes in the cerebellum. For example, schizophrenia patients have shown reduced

TABLE 2. Significant functional connectivity increases associated with structurally atrophied areas in SCA7

Seed		Regions showing significantly decreasing functional connectivity with seed				MNI (mm)		
	Anatomical location		Anatomical location	BA	mm³	X	Y	Z
Right	Lingual gyrus	Right	Semilunar posterior cerebellum		30,976	26	−70	−40
Right	Cerebellum posterior	Right	Lingual gyrus	18	18,624	26	−86	−4
Right	Lingual gyrus	Left	Inferior parietal	40	8,960	−62	−30	24
Left	Cerebellum anterior	Left	Precuneus	31	5,312	−14	−62	28
Right	Precentral gyrus	Left	Inferiror frontal gyrus	47	4,160	−46	14	−8
Left	Cerebellum posterior	Right	Middle occipital gyrus	18	3,008	26	−94	12
Left	Precentral gyrus	Right	Superior frontal gyrus	8	2,752	6	38	52
Left	Inferior occipital gyrus	Left	Inferior temporal gyrus	37	2,560	−54	−58	−4
Left	Postcentral gyrus	Right	Subcallosal gyrus	34	2,432	26	6	−16
Left	Precentral gyrus	Right	Uvula posterior cerebellum		2,176	22	−78	−36
Right	Postcentral gyrus	Left	Superior temporal gyrus	22	2,112	−50	10	−8
Left	Inferior occipital gyrus	Left	Inferior parietal	40	1,984	−54	−58	44
Left	Inferior occipital gyrus	Left	Uvula posterior cerebellum		1,984	−14	−78	−32
Right	Cerebellum anterior	Right	Tonsil posterior cerebellum		1,792	10	−54	−40
Left	Cerebellum posterior	Left	Inferior occipital gyrus	18	1,792	−34	−90	−4
Left	Precentral gyrus	Right	Thalamus		1,792	18	−18	12
Right	Cuneus	Right	Fusiform gyrus	19	1,664	38	−82	−12
Left	Postcentral gyrus	Right	Superior temporal gyrus	22	1,664	58	6	−4
Right	Cerebellum anterior	Left	Precuneus	31	1,600	−2	−46	36
Right	Cerebellum anterior	Left	Superior parietal	7	1,600	−34	−54	64
Right	Cerebellum posterior	Left	Insula	13	1,600	−38	−6	8
Right	Cerebellum anterior	Left	Inferior parietal	40	1,536	−42	−38	44
Left	Precuneus	Left	Superior temporal gyrus	22	1,472	−62	−54	20
Left	Cerebellum anterior	Left	Hippocampus		1,280	−30	−38	0
Right	Cerebellum posterior	Left	Culmen anterior cerebellum		1,280	−2	−66	−8

Coordinates represent the peak value of the cluster in Montreal Neurological Institute space in millimeters.
Brodmann areas were obtained through Talaraich Daemon.

blood oxygen level dependent (BOLD) activity in both regions, and increased regional cerebral blood flow has been reported in verbal memory tasks,[53,54] whereas functional connections between the two regions have been observed to be affected in major depression.[55] Therefore, the observed disruption in cerebellar-frontal/parahippocampal connectivity suggests certain cognitive deficits in SCA7 patients, which is consistent with previous findings of a preliminary study in which tests of intellectual and executive functioning showed impairments in SCA7 patients.[56]

Abnormality in Visual Functional Connectivity

The most important landmark that originally differentiated SCA7 from other SCAs was retinal degeneration.[11] Although retinal degeneration clearly contributes to the visual impairment in SCA7 patients, our current results, together with a previous VBM finding,[14] suggest that visual cortex degeneration and functional deterioration of the visual pathways may also contribute significantly. The reciprocal reduction of functional connectivity between the right lingual gyrus/left cuneus and bilateral post/precentral gyrus (Table 2) suggests a disruption of information flow between the visual and motor areas.[57–59] Again, gray matter volume is reduced in both the visual and motor areas in the SCA7 group. These results highlight the pervasive effect that SCA7 exerts on the visual and motor systems.[2,6,8,11] Our findings indicate that not only are these two systems individually affected, as indicated by reduced gray matter volume, but their interaction/coordination is also disrupted. Moreover, some studies have suggested that abnormal patterns in functional connectivity could precede the structural degeneration,[21,60] raising the question of whether the abnormal functional interaction is the result of the structural degeneration or if the degeneration of the visual system is caused by the abnormal patterns of functional connectivity. This finding provides another mechanism that helps to explain the frequently observed visual-motor coordination disruption in SCA7 patients,[11] but further investigation is required.

Other Abnormalities in Functional Connectivity

In addition to the areas discussed above, the posterior parietal cortex, especially the precuneus, also showed significantly reduced connectivity with the inferior frontal gyrus in the SCA7 group. The posterior part of the parietal cortex is critical for sensory-motor integration

TABLE 3. Significant functional connectivity decreases associated with structurally atrophied areas in SCA7

| Seed			Regions showing significantly decreasing functional connectivity with seed					
							MNI (mm)	
	Anatomical location		Anatomical location	BA	mm³	X	Y	Z
Right	Cerebellum posterior	Left	Superior frontal gyrus	6	20,416	−22	18	56
Right	Precuneus	Right	Inferior frontal gyrus	44	18,496	54	18	8
Right	Lingual gyrus	Right	Postcentral gyrus	3	13,312	34	−30	56
Right	Lingual gyrus	Left	Postcentral gyrus	3	11,840	−38	−22	56
Left	Precentral gyrus	Left	Lingual gyrus	18	11,520	−10	−70	0
Right	Cerebellum anterior	Right	Superior frontal gyrus	10	8,512	30	54	16
Left	Cerebellum posterior	Right	Middle frontal gyrus	9	8,192	46	26	28
Right	Cerebellum anterior	Left	Fusiform gyrus	18	5,504	−26	−90	−16
Right	Cerebellum posterior	Right	Middle frontal gyrus	6	5,440	34	10	56
Right	Lingual gyrus	Left	Middle frontal gyrus	18	4,544	−10	−94	20
Right	Postcentral gyrus	Left	Cuneus	19	4,416	−22	−90	36
Right	Precentral gyrus	Right	Superior temporal gyrus	38	4,288	34	10	−32
Right	Postcentral gyrus	Right	Cuneus	19	3,904	22	−82	36
Left	Precentral gyrus	Right	Middle occipital gyrus	18	3,328	18	−90	20
Right	Cerebellum anterior	Right	Inferior frontal gyrus	47	3,008	38	26	−4
Left	Precuneus	Left	Parahippocampal gyrus	30	2,944	−14	−46	0
Right	Cerebellum posterior	Right	Uncus	36	2,880	30	−6	−40
Right	Cerebellum posterior	Left	Superior Parietal	7	2,688	−38	−70	52
Right	Cerebellum anterior	Left	Superior frontal gyrus	10	2,368	−22	46	16
Right	Lingual gyrus	Left	Precentral gyrus	6	2,176	−42	−6	28
Right	Precentral gyrus	Right	Postcentral gyrus	1	1,984	46	−26	60
Right	Precentral gyrus	Left	Middle occipital gyrus	19	1,984	−30	−94	12
Left	Cerebellum posterior	Right	Superior frontal gyrus	6	1,920	26	14	56
Right	Precentral gyrus	Right	Lingual gyrus	17	1,728	18	−90	8
Left	Postcentral gyrus	Left	Paracentral gyrus	5	1,664	−6	−38	56
Right	Cerebellum posterior	Right	Precuneus	19	1,600	38	−74	40
Right	Cerebellum anterior	Left	Parahippocampal gyrus	20	1,536	−38	−30	−16
Right	Cerebellum posterior	Right	Middle frontal gyrus	9	1,536	46	14	36
Left	Postcentral gyrus	Left	Cuneus	19	1,472	−26	−82	32
Left	Cerebellum anterior	Right	Declive posterior cerebellum		1,344	42	−74	−16

Highlighted rows indicate regions showing negative effect of CAG repetition and years of symptom.
Coordinates represent the peak value of the cluster in Montreal Neurological Institute space in millimeters.
Brodmann areas were obtained through Talaraich Daemon.

and is highly involved with movement intention, planning, and reaching.[61,62] Deficits associated with posterior parietal connectivity would probably have significant visuospatial consequences. For example, subjects showing aberrant connectivity patterns with posterior parietal areas after stroke have spatial neglect.[63] On the other hand, the right inferior frontal gyrus has been related with go/no-go and stop signal tasks,[64–66] and lesions in this region result in impairment in performance of inhibitory control tasks.[67] Therefore, the observed disruption in functional connectivity between the precuneus and right inferior frontal gyrus might be related to deficits in integration of visual spatial information for correct decision making and inhibitory control in SCA7 patients. Aberrant anterior-posterior functional connections between parietal and frontal cortices have been found in other neurodegenerative and psychiatric disorders such as Alzheimer's disease, Huntington's disease, and autism spectrum disorders.[68–70] However, the functional connectivity changes

in SCA7 such as frontocerebellar and visuomotor disruption seem to be more disease specific, supporting the theory that neurodegenerative diseases target specific regions in large-scale networks.[21]

Effects of CAG Expansion and Number of Years After Onset on Functional Connectivity

Various studies have documented the association between gene mutation and functional connectivity in different brain disorders. For example, deficits in functional connectivity in prodromal Huntington's disease associated with depressive symptoms were correlated with effects of the CAG repetition in the Huntingtin allele.[71] Moreover, the D-amino acid oxidase activator gene was reported to affect the homogeneity of functional connectivity patterns in major depressive disorder.[72] Therefore, we expected similar correlations between functional connectivity and number of trinucleotide repeats in our SCA7 patient population. Indeed,
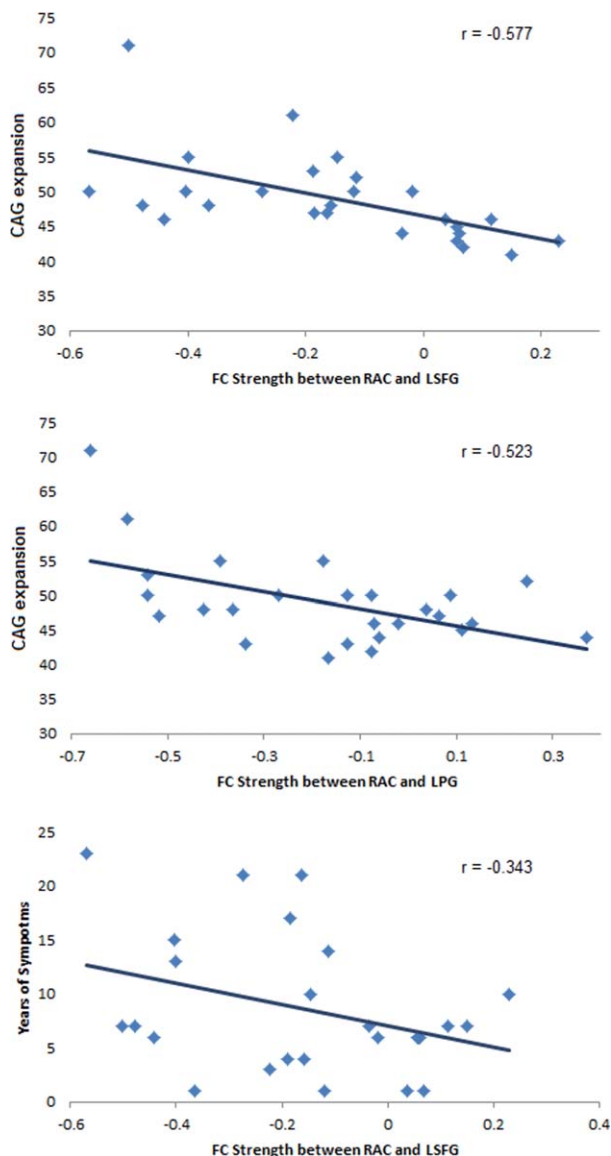
FIG. 2. Graphic representation of the relationship between CAG expansion and functional connectivity (FC) strength between right anterior cerebellum (RAC) and left superior frontal gyrus (LSFG), top, CAG expansion and FC strength between right anterior cerebellum and left parahippocampal gyrus (LPG), center, and years of symptoms and FC strength between right anterior cerebellum and left superior frontal gyrus (bottom). For each scatter plot, the *y* axis represents the behavioral score and the *x* axis the functional connectivity value between two regions. [Color figure can be viewed in the online issue, which is available at wileyonlinelibrary.com.]

our analyses found that CAG expansion had a negative effect on functional connectivity between the cerebellum and the superior frontal gyrus and between the cerebellum and the parahippocampal gyrus. The number of years after onset also showed a correlation trend ($P = 0.01$ uncorrected) with the functional connectivity between the cerebellum and the superior frontal gyrus. Although not conclusive, these results suggest that the gene/symptom-connectivity correlation has major relevance in the association between the cerebellum and

higher-order brain areas related to memory and executive control.[73–76] Nevertheless, that the severity of the genetic mutation does not show significant correlation with more prevalent abnormalities in visual/motor functional connectivity deserves further investigation.

Limitations

This study applied VBM analysis to detect functional abnormalities associated with structural deficits in SCA7 patients. Criticisms of the use of VBM have been made,[77] arguing that the method suffers when the images are low quality, but it also has been shown to function well with properly acquired data.[78] Such combined VBM and functional connectivity analysis has been implemented successfully in previous studies,[79] and in this study we placed 12 seeds in the most affected brain areas to ensure the strictness of the data. However, it is possible that abnormalities in functional connectivity could arise in the absence of structural deficits, which deserves further investigation. Another limitation of the present study was the lack of detailed behavioral and cognitive characterization of SCA7 patients, for example, the combined effect of age difference and years since onset. The absence of such data precludes possible correlational analyses that could have further clarified the observed functional connectivity abnormalities.

Conclusions

The combined anatomical and functional connectivity analysis of SCA7 patients revealed widespread functional connectivity abnormalities, especially within the cerebellar, visual, and motor cortical systems. Our results also indicate a potential quantitative relationship between mutation expansion and functional connectivity abnormalities. Finally, our data revealed multiple functional connectivity deficits in various higher-order cognitive areas including the parahippocampal gyrus and different frontal areas that have not been previously reported. Although memory and other cognitive capacities related to SCA7 need to be explored, our results provide novel and relevant information for the understanding of SCA7 disease. ∎

References

1. Garden GA, La Spada AR. Molecular pathogenesis and cellular pathology of spinocerebellar ataxia type 7 neurodegeneration. Cerebellum. 2008;7:138–149.

2. Hugosson T, Granse L, Ponjavic V, Andreasson S. Macular dysfunction and morphology in spinocerebellar ataxia type 7 (SCA 7). Ophthalmic Genet. 2009;30:1–6.

3. David G, Durr A, Stevanin G, et al. Molecular and clinical correlations in autosomal dominant cerebellar ataxia with progressive macular dystrophy (SCA7). Hum Mol Genet. 1998;7:165–170.

4. Johansson J, Forsgren L, Sandgren O, Brice A, Holmgren G, Holmberg M. Expanded CAG repeats in Swedish spinocerebellar ataxia type 7 (SCA7) patients: effect of CAG repeat length on the clinical manifestation. Hum Mol Genet. 1998;7:171–176.

5. Martin JJ. Spinocerebellar ataxia type 7. Handb Clin Neurol. 2012;103:475–491.

6. Miller RC, Tewari A, Miller JA, Garbern J, Van Stavern GP. Neuro-ophthalmologic features of spinocerebellar ataxia type 7. J Neuroophthalmol. 2009;29:180–186.

7. Paulson HL. The spinocerebellar ataxias. J Neuroophthalmol. 2009;29:227–237.

8. Michalik A, Martin JJ, Van Broeckhoven C. Spinocerebellar ataxia type 7 associated with pigmentary retinal dystrophy. Eur J Hum Genet. 2004;12:2–15.

9. Masciullo M, Modoni A, Pomponi MG, et al. Evidence of white matter involvement in SCA 7. J Neurol. 2007;254:536–538.

10. Enevoldsen TP, Sanders MD, Harding AE. Autosomal dominant cerebellar ataxia with pigmentary macular dystrophy. A clinical and genetic study of eight families. Brain. 1994;117:445–460.

11. Gouw LG, Digre KB, Harris CP, Haines JH, Ptacek LJ. Autosomal dominant cerebellar ataxia with retinal degeneration: clinical, neuropathologic, and genetic analysis of a large kindred. Neurology. 1994;44:1441–1447.

12. Dohlinger S, Hauser TK, Borkert J, Luft AR, Schulz JB. Magnetic resonance imaging in spinocerebellar ataxias. Cerebellum. 2008;7:204–214.

13. Bang OY, Lee PH, Kim SY, Kim HJ, Huh K. Pontine atrophy precedes cerebellar degeneration in spinocerebellar ataxia 7: MRI-based volumetric analysis. J Neurol Neurosurg Psychiatry. 2004;75:1452–1456.

14. Alcauter S, Barrios FA, Diaz R, Fernandez-Ruiz J. Gray and white matter alterations in spinocerebellar ataxia type 7: an in vivo DTI and VBM study. Neuroimage. 2011;55:1–7.

15. Wang L, Roe CM, Snyder AZ, et al. Alzheimer disease family history impacts resting state functional connectivity. Ann Neurol. 2012;72:571–577.

16. Hacker CD, Perlmutter JS, Criswell SR, Ances BM, Snyder AZ. Resting state functional connectivity of the striatum in Parkinson's disease. Brain. 2012;135:3699–3711.

17. Reetz K, Dogan I, Rolfs A, et al. Investigating function and connectivity of morphometric findings--exemplified on cerebellar atrophy in spinocerebellar ataxia 17 (SCA17). Neuroimage. 2012;62:1354–1366.

18. Wu T, Wang C, Wang J, Hallett M, Zang Y, Chan P. Preclinical and clinical neural network changes in SCA2 parkinsonism. Parkinsonism Relat Disord. 2013;19:158–164.

19. Solodkin A, Peri E, Chen EE, Ben-Jacob E, Gomez CM. Loss of intrinsic organization of cerebellar networks in spinocerebellar ataxia type 1: correlates with disease severity and duration. Cerebellum. 2011;10:218–232.

20. Biswal B, Yetkin FZ, Haughton VM, Hyde JS. Functional connectivity in the motor cortex of resting human brain using echo-planar MRI. Magn Reson Med. 1995;34:537–541.

21. Seeley WW, Crawford RK, Zhou J, Miller BL, Greicius MD. Neurodegenerative diseases target large-scale human brain networks. Neuron. 2009;62:42–52.

22. Greicius M. Resting-state functional connectivity in neuropsychiatric disorders. Curr Opin Neurol. 2008;21:424–430.

23. Cherkassky VL, Kana RK, Keller TA, Just MA. Functional connectivity in a baseline resting-state network in autism. Neuroreport. 2006;17:1687–1690.

24. Kennedy DP, Courchesne E. The intrinsic functional organization of the brain is altered in autism. Neuroimage. 2008;39:1877–1885.

25. Greicius MD, Srivastava G, Reiss AL, Menon V. Default-mode network activity distinguishes Alzheimer's disease from healthy aging: evidence from functional MRI. Proc Natl Acad Sci USA. 2004;101:4637–4642.

26. He Y, Wang L, Zang Y, et al. Regional coherence changes in the early stages of Alzheimer's disease: a combined structural and resting-state functional MRI study. Neuroimage. 2007;35:488–500.

27. Sorg C, Riedl V, Muhlau M, et al. Selective changes of resting-state networks in individuals at risk for Alzheimer's disease. Proc Natl Acad Sci USA. 2007;104:18760–18765.

28. Wang L, Zang Y, He Y, et al. Changes in hippocampal connectivity in the early stages of Alzheimer's disease: evidence from resting state fMRI. Neuroimage. 2006;31:496–504.

29. Wang K, Liang M, Wang L, et al. Altered functional connectivity in early Alzheimer's disease: a resting-state fMRI study. Hum Brain Mapp. 2007;28:967–978.

30. Liang M, Zhou Y, Jiang T, et al. Widespread functional disconnectivity in schizophrenia with resting-state functional magnetic resonance imaging. Neuroreport. 2006;17:209–213.

31. Alonso E, Martinez-Ruano L, De Biase I, et al. Distinct distribution of autosomal dominant spinocerebellar ataxia in the Mexican population. Mov Disord. 2007;22:1050–1053.

32. Fox MD, Corbetta M, Snyder AZ, Vincent JL, Raichle ME. Spontaneous neuronal activity distinguishes human dorsal and ventral attention systems. Proc Natl Acad Sci USA. 2006;103:10046–10051.

33. Power JD, Barnes KA, Snyder AZ, Schlaggar BL, Petersen SE. Spurious but systematic correlations in functional connectivity MRI networks arise from subject motion. Neuroimage. 2012;59:2142–2154.

34. Jenkinson M, Bannister P, Brady M, Smith S. Improved optimization for the robust and accurate linear registration and motion correction of brain images. Neuroimage. 2002;17:825–841.

35. Jenkinson M, Smith S. A global optimisation method for robust affine registration of brain images. Med Image Anal. 2001;5:143–156.

36. Rueckert D, Sonoda LI, Hayes C, Hill DL, Leach MO, Hawkes DJ. Nonrigid registration using free-form deformations: application to breast MR images. IEEE Trans Med Imaging. 1999;18:712–721.

37. Ashburner J, Friston KJ. Voxel-based morphometry—the methods. Neuroimage. 2000;11:805–821.

38. Good CD, Johnsrude IS, Ashburner J, Henson RN, Friston KJ, Frackowiak RS. A voxel-based morphometric study of ageing in 465 normal adult human brains. Neuroimage. 2001;14:21–36.

39. Smith SM, Jenkinson M, Woolrich MW, et al. Advances in functional and structural MR image analysis and implementation as FSL. Neuroimage. 2004;23(Suppl 1):S208–S219.

40. Hayasaka S, Nichols TE. Combining voxel intensity and cluster extent with permutation test framework. Neuroimage. 2004;23:54–63.

41. Nichols TE, Holmes AP. Nonparametric permutation tests for functional neuroimaging: a primer with examples. Hum Brain Mapp. 2002;15:1–25.

42. Poline JB, Worsley KJ, Evans AC, Friston KJ. Combining spatial extent and peak intensity to test for activations in functional imaging. Neuroimage. 1997;5:83–96.

43. Middleton FA, Strick PL. The cerebellum: an overview. Trends Neurosci. 1998;21:367–369.

44. Schmahmann JD. Dysmetria of thought: clinical consequences of cerebellar dysfunction on cognition and affect. Trends Cogn Sci. 1998;2:362–371.

45. Desmond JE, Fiez JA. Neuroimaging studies of the cerebellum: language, learning and memory. Trends Cogn Sci. 1998;2:355–362.

46. Rytsar R, Fornari E, Frackowiak RS, Ghika JA, Knyazeva MG. Inhibition in early Alzheimer's disease: an fMRI-based study of effective connectivity. Neuroimage. 2011;57:1131–1139.

47. Qiu A, Tuan TA, Woon PS, Abdul-Rahman MF, Graham S, Sim K. Hippocampal-cortical structural connectivity disruptions in schizophrenia: an integrated perspective from hippocampal shape, cortical thickness, and integrity of white matter bundles. Neuroimage. 2010;52:1181–1189.

48. Liang P, Wang Z, Yang Y, Jia X, Li K. Functional disconnection and compensation in mild cognitive impairment: evidence from DLPFC connectivity using resting-state fMRI. PLoS One 2011;6:e22153.

49. Bullmore E, Sporns O. Complex brain networks: graph theoretical analysis of structural and functional systems. Nat Rev Neurosci. 2009;10:186–198.

50. Maguire EA, Burgess N, Donnett JG, Frackowiak RS, Frith CD, O'Keefe J. Knowing where and getting there: a human navigation network. Science. 1998;280:921–924.

51. O'Reilly JX, Beckmann CF, Tomassini V, Ramnani N, Johansen-Berg H. Distinct and overlapping functional zones in the cerebellum defined by resting state functional connectivity. Cereb Cortex. 2010;20:953–965.

52. Krienen FM, Buckner RL. Segregated fronto-cerebellar circuits revealed by intrinsic functional connectivity. Cereb Cortex. 2009;19:2485–2497.

53. Grasby PM, Frith CD, Friston KJ, Bench C, Frackowiak RS, Dolan RJ. Functional mapping of brain areas implicated in auditory--verbal memory function. Brain. 1993;116:1–20.

54. Shergill SS, Brammer MJ, Fukuda R, Williams SC, Murray RM, McGuire PK. Engagement of brain areas implicated in processing inner speech in people with auditory hallucinations. Br J Psychiatry. 2003;182:525–531.

55. Zeng LL, Shen H, Liu L, et al. Identifying major depression using whole-brain functional connectivity: a multivariate pattern analysis. Brain. 2012;135:1498–1507.

56. Sokolovsky N, Cook A, Hunt H, Giunti P, Cipolotti L. A preliminary characterisation of cognition and social cognition in spinocerebellar ataxia types 2, 1, and 7. Behav Neurol. 2010;23:17–29.

57. Glickstein M. How are visual areas of the brain connected to motor areas for the sensory guidance of movement? Trends Neurosci. 2000;23:613–617.

58. Myers RE, Sperry RW, Mc CN. Neural mechanisms in visual guidance of limb movement. Arch Neurol. 1962;7:195–202.

59. Macaluso E, Frith CD, Driver J. Modulation of human visual cortex by crossmodal spatial attention. Science. 2000;289:1206–1208.

60. Zhou J, Gennatas ED, Kramer JH, Miller BL, Seeley WW. Predicting regional neurodegeneration from the healthy brain functional connectome. Neuron. 2012;73:1216–1227.

61. Astafiev SV, Shulman GL, Stanley CM, Snyder AZ, Van Essen DC, Corbetta M. Functional organization of human intraparietal and frontal cortex for attending, looking, and pointing. J Neurosci. 2003;23:4689–4699.

62. Fernandez-Ruiz J, Goltz HC, DeSouza JF, Vilis T, Crawford JD. Human parietal "reach region" primarily encodes intrinsic visual direction, not extrinsic movement direction, in a visual motor dissociation task. Cereb Cortex. 2007;17:2283–2292.

63. He BJ, Snyder AZ, Vincent JL, Epstein A, Shulman GL, Corbetta M. Breakdown of functional connectivity in frontoparietal networks underlies behavioral deficits in spatial neglect. Neuron. 2007;53:905–918.

64. Aron AR, Robbins TW, Poldrack RA. Inhibition and the right inferior frontal cortex. Trends Cogn Sci. 2004;8:170–177.

65. Garavan H, Ross TJ, Stein EA. Right hemispheric dominance of inhibitory control: an event-related functional MRI study. Proc Natl Acad Sci U S A. 1999;96:8301–8306.

66. Konishi S, Nakajima K, Uchida I, Kikyo H, Kameyama M, Miyashita Y. Common inhibitory mechanism in human inferior prefrontal cortex revealed by event-related functional MRI. Brain. 1999;122:981–991.

67. Aron AR, Fletcher PC, Bullmore ET, Sahakian BJ, Robbins TW. Stop-signal inhibition disrupted by damage to right inferior frontal gyrus in humans. Nat Neurosci. 2003;6:115–116.

68. Wolf RC, Sambataro F, Vasic N, Shonfeldt-Lecuona C, Ecker D, Landwehrmeyer B. Aberrant connectivity of lateral prefrontal networks in presymptomatic Huntington's disease. Exp Neurol. 2008;213:137–144.

69. Wang K, Liang M, Wang L, et al. Altered functional connectivity in early Alzheimer's disease: a resting-state fMRI study. Hum Brain Mapp. 2007;28:967–978.

70. Perez Velazquez JL, Barcelo F, Hung Y, et al. Decreased brain coordinated activity in autism spectrum disorders during executive tasks: reduced long-range synchronization in the fronto-parietal networks. Int J Psychophysiol. 2009;73:341–349.

71. Unschuld PG, Joel SE, Pekar JJ, et al. Depressive symptoms in prodromal Huntington's Disease correlate with Stroop-interference related functional connectivity in the ventromedial prefrontal cortex. Psychiatry Res. 2012;203:166–174.

72. Chen J, Xu Y, Zhang J, et al. Genotypic association of the DAOA gene with resting-state brain activity in major depression. Mol Neurobiol. 2012;46:361–373.

73. Schmahmann JD, Sherman JC. The cerebellar cognitive affective syndrome. Brain. 1998;121:561–579.

74. Timmann D, Daum I. Cerebellar contributions to cognitive functions: a progress report after two decades of research. Cerebellum. 2007;6:159–162.

75. Tedesco AM, Chiricozzi FR, Clausi S, Lupo M, Molinari M, Leggio MG. The cerebellar cognitive profile. Brain. 2011;134:3672–3686.

76. Stoodley CJ, Valera EM, Schmahmann JD. Functional topography of the cerebellum for motor and cognitive tasks: an fMRI study. Neuroimage. 2012;591560–1570.

77. Bookstein FL. "Voxel-based morphometry" should not be used with imperfectly registered images. Neuroimage. 2001;14:1454–1462.

78. Ashburner J, Friston KJ. Why voxel-based morphometry should be used. Neuroimage. 2001;14:1238–1243.

79. Ye T, Peng J, Nie B, et al. Altered functional connectivity of the dorsolateral prefrontal cortex in first-episode patients with major depressive disorder. Eur J Radiol. 2012;81:4035–4040.